1   *Article*

2   # Design, synthesis and *in combo* antidiabetic

3   # bioevaluation of multitarget phenylpropanoic acids[¥]

4   **Blanca Colín-Lozano[1], Samuel Estrada-Soto[1], Fabiola Chávez-Silva[1], Abraham Gutiérrez-Hernández[1],**
5   **Litzia Cerón-Romero[1], Abraham Giacoman-Martínez[2], Julio Cesar Almanza-Pérez[2], Emanuel**
6   **Hernández-Núñez[3], Zhilong Wang[4], Xin Xie[4], Mario Cappiello[5], Francesco Balestri[5], Umberto Mura[5],**
7   **and Gabriel Navarrete Vázquez [1,*]**

8   [1] Facultad de Farmacia, Universidad Autónoma del Estado de Morelos, Cuernavaca, Morelos, 62209, México;
9   clbi_ff@uaem.mx (B.C.-L); enoch@uaem.mx (S.E.-S.); facasy@gmail.com (F.C.-S.); ghaa_ff@uaem.mx
10   (A.G.-H.); crlc_ff@uaem.mx (L. C.-R); gabriel_navarrete@uaem.mx (G.N.-V)
11   [2] Laboratorio de Farmacología, Depto. Ciencias de la Salud, Universidad Autónoma Metropolitana-Iztapalapa,
12   09340, D.F. México; agmfest@hotmail.com (A.G.-M); j.almanza.perez@gmail.com (JC A.-P.)
13   [3] Cátedra CONACyT, Departamento de Recursos del Mar, Centro de Investigación y de Estudios Avanzados del
14   IPN, Unidad Mérida, 97310, Yucatán, México; emanuel.hernandez@cinvestav.mx (E.H.-N.)
15   [4] CAS Key Laboratory of Receptor Research, the National Center for Drug Screening, Shanghai Institute of Materia
16   Medica, Chinese Academy of Sciences, Shanghai 201203, China. endlesslily@hotmail.com (X.W.);
17   xxie@simm.ac.cn (X.X.)
18   [5] Dipartimento di Biologia, Unità di Biochimica, University of Pisa, Pisa, 56126, Italy;
19   mcappiello@biologia.unipi.it (M.C.); francesco.balestri@unipi.it (F.B.); umberto.mura@unipi.it (U.M.)
20
21   * Correspondence e-mail: gabriel_navarrete@uaem.mx; Tel.: +52-777-329-7089
22   ¥ Taking in part of the Ph. D. thesis of B. Colín-Lozano

23

24   **Abstract:** We synthesized a small series of five 3-[4-arylmethoxy)phenyl]propanoic acids using an easy
25   and short step synthetic route. All compounds were tested *in vitro* against a set of four protein targets
26   identified as key elements in diabetes: GPR40, aldose reductase (AKR1B1), PPARγ and GLUT-4.
27   Compound **1** displayed an EC_{50} value of 0.075 μM against GPR40 and was an AKR1B1 inhibitor, showing
28   $IC_{50} = 7.4$ μM. Compounds **2** and **3** behave as AKR1B1 inhibitors, GPR40 agonists and showed an increase
29   of 2 to 4-times in the mRNA expression of PPARγ, as well as the GLUT-4 levels. Docking studies were
30   conducted in order to explain the polypharmacological mode of action and the interaction binding mode
31   of the most active compounds on these targets. Compounds **1-3** were tested *in vivo* at 100 mg/kg dose,
32   being **2** and **3** orally actives, reducing glucose levels in a non insulin-dependent diabetes mellitus mice
33   model. Compounds **2** and **3** showed robust *in vitro* and *in vivo* efficacy, and could be considered as
34   promising multitarget antidiabetic drug candidates. This is the first report of a single molecule with these
35   four polypharmacological target action.

36

37   **Keywords:** Diabetes; GPR40; AKRB1; PPARγ, GLUT-4

38

39

1. Introduction

Diabetes Mellitus (DM) is a multifactorial metabolic disease that occurs with fasting blood glucose concentrations above 120 mg/dL (>7 mM), due to the abnormal pancreatic β-cells and/or insulin resistance. The susceptibility to environmental influences, and immune dysregulation or inflammation, lead to the variety of hyperglycemic phenotypes within the spectrum of DM [1]. Currently, experimental drug discovery for Type 2 Diabetes Mellitus (T2DM) is focused on developing drugs for insulin sensitizing and/or releasing effect by several mechanisms. One of them is mediated by the G protein-coupled receptor 40 (GPR40, also known as FFA1), which is primarily expressed in pancreatic β-cells and enteroendocrine cells of the gut [2, 3]. The GPR40 activation by medium to long chain fatty acids, stimulates insulin secretion only in the presence of elevated glucose concentration but does not affect insulin exocytosis at low glucose levels [4, 5]. This intriguing mechanism was suggestive in treating T2DM by small molecules agonists for GPR40, thus playing as novel insulin secretagogues with little or no risk of hypoglycemia [6]. An alternative mechanism for the control of glucose levels refers to the peroxisome proliferator-activated receptors (PPARs) action. PPARs, members of the nuclear hormone receptor superfamily, belonging to the ligand activated transcription factors that occur in three subtypes: PPARα, PPARγ, and PPARβ/δ [7]. Each subtype regulates tissue-specific target genes acting as lipid sensors and regulators of glucose homeostasis, such as the solute carrier family 2 (facilitated glucose transporter), member 4 (GLUT-4) [8]. Thiazolidine-2,4-diones function as insulin-sensitizing drugs, through the activation of PPARγ [9, 10], leading to enforced expression of target genes involved in glucose-sensing ability of pancreatic β-cells in diabetic subjects [11]. On the other hand, prolonged hyperglycemia plays a significant role in the development of diabetic complications such as atherosclerosis, neuropathy, end stage renal failure and blindness. The NADPH-dependent reduction of elevated levels of D-glucose to sorbitol catalyzed by aldose reductase (AKR1B1) is considered as one of the phenomena leading to the onset of long term diabetic complications [12]. Stressful and damaging cell conditions are produced by several factors such as the osmotic imbalance due to sorbitol accumulation, the loss of antioxidant power related with NADPH oxidation and the induction of additional advantageous conditions for protein glycation [13-15]. Inhibition of AKR1B1 represents a potential target of antidiabetic drug action. The purpose of the present work was to design, synthesize and screen *in vitro*, *in vivo* and *in silico* (*in combo* screens) a small series of five 3-[4-arylmethoxy)phenyl]propanoic acids to achieve the treatment of diabetes with a single molecule with multitarget action: activation of PPARγ, GLUT-4 and GPR40 and inhibition of AKR1B1 (Figure 1). This multitarget therapy may be an attractive option for the therapeutic treatment of diabetes that will not only control the glucose level but also reduce acute complications linked to hyperglycemic conditions.
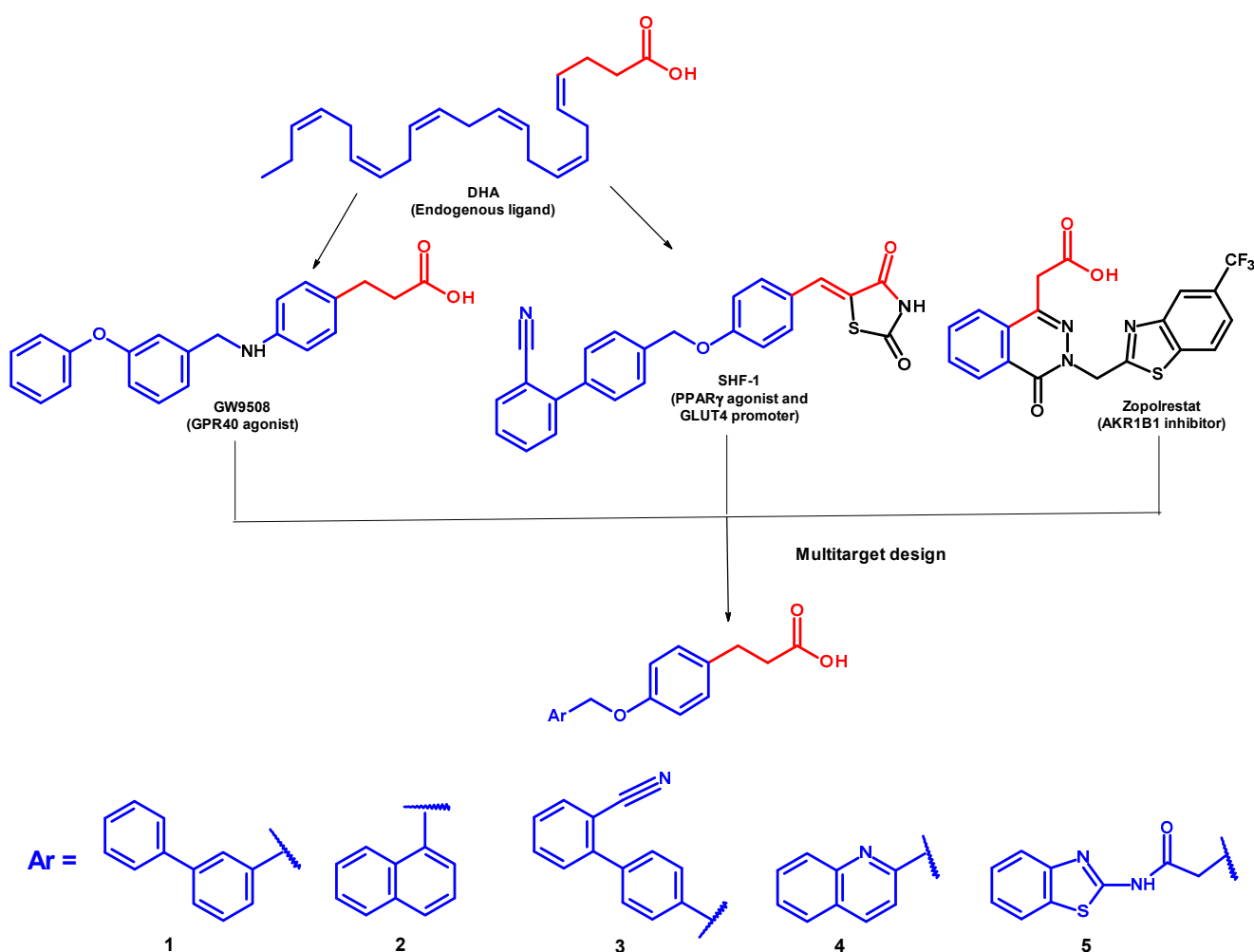
78
79
80
81
82
83
84
85
86
87
88
89
90
91
92
93
94
95
96
97
98
99
100

101 **Figure 1.**   Drug design of multitarget compounds **1–5**, which were designed from pharmacophore
102 extraction and reorganization from known modulators of four targets: GPR40, PPARγ, GLUT-4, and
103 AKR1B1.

2.   Results and Discussion

2.1. Drug design of derivatives 1–5

106 Compounds **1–5** were designed on the basis of the structure of the compounds **GW9508** [16] and **SHF-1**
107 [17], maintaining the typical 4-point pharmacophore of synthetic GPR40 agonists [6], that mimic the fatty
108 acid structure of endogenous agonists (Figure 1): (I) An acidic group (carboxylic acid or related
109 bioisosteres); (II) A central aromatic ring; (III) An extra-lipophilic region and (IV) a flexible spacer that
110 connects regions (I) and (IV), and tolerating the structure to adopt diverse conformations. The insulin-
111 sensitizer targets PPARγ and GPR40 which are activated by long chain fatty acids and thiazolidine-2,4-
112 diones are described to function as an integrated two-receptor signal transduction pathway [18] being
113 sensitive to closely related pharmacophores, as represented by **GW9508** and **SHF-1** [17]. Then, it is
114 reasonable to assume that also compounds **1-5** may act as agonists on these targets in a similar fashion.

115 On the other hand, carboxylic acid derivatives comprise the majority of reported AKR1B1 inhibitors:
116 epalrestat, tolrestat and zopolrestat. The other two chemical groups that function as inhibitors are:
117 spirohydantoins (Sorbinil) and flavonoids such as quercetin [19]. Based on the relevance of the
118 phenylpropanoic scaffold (Fig. 1) in determining the inhibitory ability of zopolrestat towards AKR1B1,
119 we expect that also compounds **1-5** may act as inhibitors of the enzyme. Due to the multifactorial
120 complexity of chronic diseases, the current therapeutic arsenal and the old-fashioned ''one-molecule,
121 one-target'' model seem not so effective [20]. The design of new chemical entities (NCE) with two or more
122 complementary bioactivities for the treatment of complex diseases would be very advantageous. Based
123 on the above considerations, our work was focused on the rational design, synthesis and evaluation of
124 these novel multitarget molecules to be active against Diabetes. Although compound **1** was previously
125 synthesized [21, 22], in the current work the effectiveness as GPR40 agonist of this compound and of the
126 accompanying molecules is extended and explored *in vivo.* A parallel investigation on the potential
127 antidiabetic action of these compounds: the activation of PPARγ and GLUT-4 and the inhibition of
128 AKR1B1, is also reported for first time. To our knowledge, this is the first study reporting the potential
129 of the simultaneous targeting of these four relevant processes linked to the diabetic pathology by a single
130 molecule.

131 **2.2. Chemistry**

132 Compounds **1-5** were prepared starting from 4-hydroxybenzaldehyde (**6**), which was condensed with
133 malonic acid (**7**), following by microwave Knoevenagel reaction and decarboxylation conditions to give
134 compound **8**. This compound was reduced under catalytic hydrogenation with 10% Pd/C affording 3-(4-
135 hydroxyphenyl)propanoic acid (**9**), which was reacted via esterification with thionyl chloride and ethanol
136 as solvent, obtaining ethyl 3-(4-hydroxyphenyl)propanoate (**10**). Subsequently, **10** was reacted with the
137 appropriately substituted methylaryl halide in polar aprotic solvents and potassium carbonate to give
138 compounds **11-14**. All were treated separately by basic hydrolysis with potassium hydroxide, to give **1-**
139 **4** (Scheme 1). Compound **5** was obtained by direct SN2 reaction between acid **9** and *N*-1,3-benzothiazol-
140 2-yl-2-chloroacetamide **(15)**. Title compounds were recovered with 51–95% yields and purified by
141 recrystallization or by column chromatography. Their chemical structures were confirmed by
142 spectroscopic (1D and 2D NMR) and spectrometric data, and their purity determined by microanalysis.
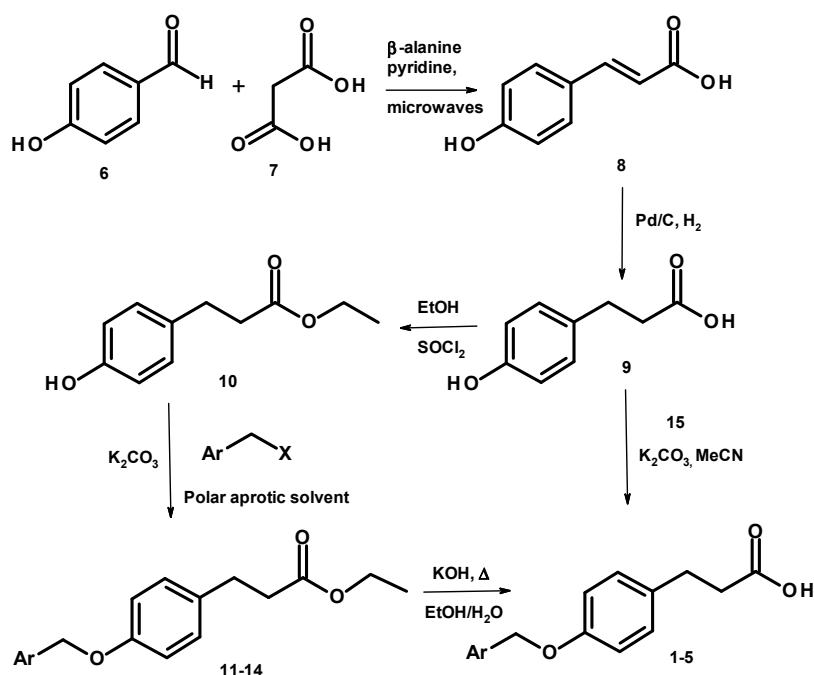
Scheme 1. Synthesis of compounds **1** -**5**

2.3. *In vitro* GPR40 activity

Compounds **1–5** were tested *in vitro* as GPR40 agonist. This activity was measured with calcium flux assay in GPR40-transfected HEK293 cells [2, 23]. The preliminary screening results are summarized in Table 1. Linoleic acid (LA), one of the endogenous ligands for GPR40, was selected as positive control. Compounds were tested in quadruplicates at 100 μM. After preliminary screening, compounds **1-5** were further tested in a concentration-dependent manner (Table 1).

Table 1.   Preliminary screening (Efficacy) and GPR40 agonistic activities (Potency) of compounds **1** -**5** in calcium assay for hGPR40/Gα16/HEK293

Comp.	Max Response % (100 μM)	EC$_{50}$ (μM)[a]
1	98±10	0.075 ±0.02
2	103±3	0.648±0.10
3	105±15	0.797±0.17
4	84	≈100
5	9.9	>100
LA	100	8.30± 1.7

[a] Calcium flux assay in GPR40-transfected HEK293 cells. Means of two experiments.

As we expected, the results indicated that compound **1** was the most potent agonist, in accordance with the literature [21, 22], followed by compounds **2** and **3,** with naphthyl and biphenylcarbonitrile substituents, respectively. All of them showed potencies in the nanomolar order. Compound **4**, with a

158   quinolynyl substituent, provided a significant decrease in agonistic activity. Conversely, benzothiazole

159   derivative **5** was inactive. It is noteworthy that the potency of compounds **1-3** is orders of magnitude

160   greater than that obtained by endogenous fatty acid ligand LA.

161   ***2.4. In vitro aldose reductase (AKR1B1) inhibition***

162   The *in vitro* AKR1B1 inhibitory activity of compounds **1-5** (Table 2) was evaluated by using a highly

163   purified human recombinant enzyme preparation [24, 25]. Sorbinil was employed as reference drug.

164   **Table 2**. Inhibition of human recombinant AKR1B1 by compounds **1-5**

Comp.	IC_{50} (μM)[a]
1	8.9 (6.5 - 12.1)
2	17.4 (14.3 - 21.2)
3	21.0 (12.8 – 34.3)
4	31.7 (22.3 - 44.9)
5	23.3 (19.0 - 25.5)
Sorbinil	1.2 (0.9 - 1.5)

165   [a] 95% confidence intervals are reported in brackets.

166   Compounds tested were shown to be generally interesting AKR1B1 inhibitors reaching up to low

167   micromolar IC_{50} values. Once again, compound **1**, previously identified as GPR40 agonist, was the most

168   active inhibitor of the series, finding this new activity for this known compound. Compound **2** was the

169   second most active, followed by compound **3** and benzothiazole **5**. Compound **4** was the least active.

170   None of them were more active than sorbinil, a well-known AKR1B1 inhibitor. As we described

171   previously, AKR1B1 plays a critical role in the development of chronic diabetic complications, such as

172   retinopathy, nephropathy, neuropathy and also cardiovascular risk. Consequently, this enzyme has been

173   presumed as an attractive target to prevent or even treat these pathologies which are a serious health

174   hazard for diabetic patients.

175   **2.5. Relative expression of PPARγ and GLUT-4**

176   To determine the effect of compounds on PPARγ and GLUT-4 expression, 3T3-L1 fibroblasts were

177   differentiated to the adipocyte phenotype. After that, cells were treated during 24 h with compounds **1-**

178   **5** and pioglitazone (10 μM) as reference drug and the mRNA expression level evaluated. Results

179   presented in Figure 2 shows that only compounds **2** and **3** increase significantly the levels of relative

180   expression for PPARγ (about three to four-times) and GLUT-4 mRNA's in the same way as pioglitazone.

181   The activation of PPARγ could decrease the glucose serum levels in diabetic patients' due to the reduction

182   in insulin resistance. Our data also suggest that compounds **2** and **3** induces GLUT-4 expression in the

183   same way than pioglitazone does. Several evidences indicate that the levels of GLUT-4 expression in

184   skeletal muscle are crucial for the regulation of total body glucose homeostasis [7, 17, 26].
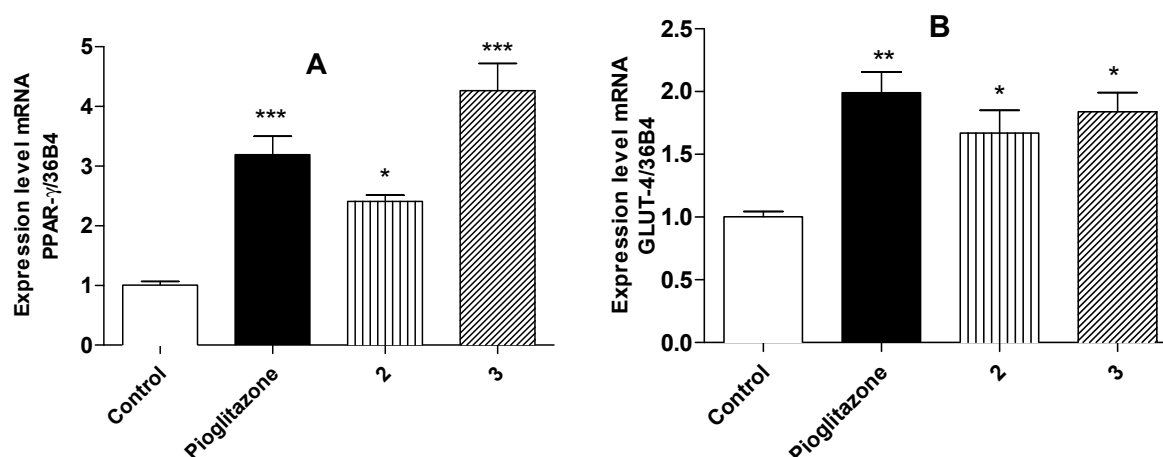
Figure 2. (A) Effect of compounds **2** and **3** on expression of mRNA PPARγ. (B) Effect of compounds on expression of mRNA GLUT-4. Results are mean ± SEM (n = 6)/***p < 0.001; ** p < 0.01; *p < 0.05 compared with control group.

2.6. Molecular docking studies

Based on the *in vitro* biological assays and the preliminary enzyme inhibition evaluations, the most active compounds were selected to explain the experimental activities on these relevant targets. On this basis, a preliminary molecular docking study was conducted to evaluate the putative binding mode of compounds **1-5** into the receptors GPR40, PPARγ and the enzyme AKR1B1. A pilot *in silico* calculation was done using DIA-DB [27], a web server for the prediction of antidiabetic drugs via inverse virtual screening of the input molecules **1-5** against a set of 18 protein targets identified as key elements in diabetes, within which are included PPARγ, GPR40 and AKR1B1, among others [28]. Subsequently, a more specific and refined analysis was carried out for the most active compounds (**1-3)**.

Refined molecular docking reveals that compounds **2** and **3** internalize into the ligand binding site of PPARγ and interact by electrostatic and hydrogen bonds with Ser-289, His-323, His-449 and Tyr-473, all of them essential for the activation of this receptor. However, compound **3** (the most active *in vitro*) showed an additional interaction with Ser-342 (Figure 3). For didactic purpose, the binding mode analysis of compound **1** was analyzed and it shows interactions with residues that are outside from the ligand binding site, which could explain its *in vitro* inactivity.
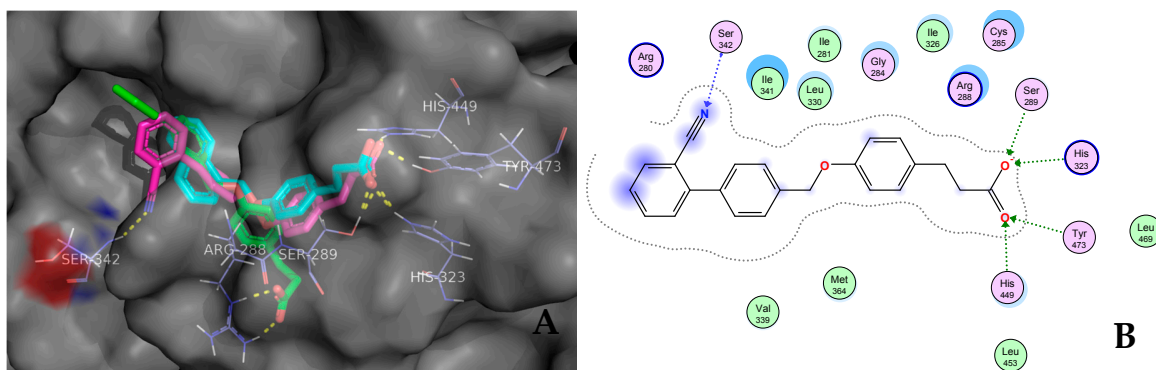
207

Figure 3. (A) 3D binding model of compounds **1-3** into the ligand binding site of PPARγ. Compounds **1** (green), **2** (cyan) and **3** (magenta) are shown as stick models, whereas aminoacids are depicted as lines. A dashed line represents polar interactions. (B) 2D interaction map of the most active compound **3** and PPARγ.

For GPR40, binding poses depicted in Figure 4 suggest that the *in vitro* active compounds **1**, **2** and **3** interact through electrostatic bonds with residues of Arg-183 and Arg-2258, and by hydrogen bonds with Tyr-91, Asn-2244, Tyr-2240, all of them showed by well-known GPR40 allosteric agonists (such as TAK-875). On the other hand, the disposition of the biphenyl ring in **1**, which was the most potent in the *in vitro* screening, fits into the GPR40 ligand-binding-*pocket* better than the other compounds generating π–π interactions with Phe-142 (Figure 4B).
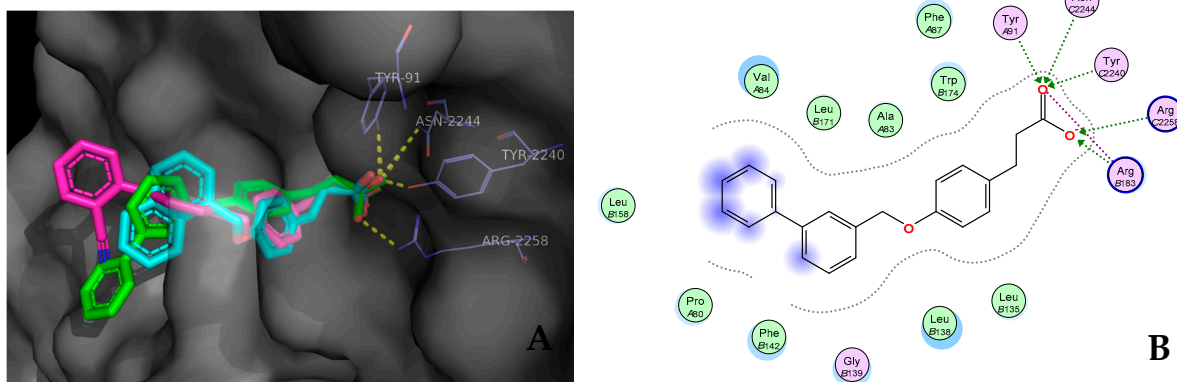

220   **Figure 4.** 3D binding model of compounds **1-3** into the allosteric ligand binding site of GPR40. Compounds **1** (green), **2** (cyan) and **3** (magenta) are shown as stick models, whereas aminoacids are depicted as lines. A dashed line represents polar interactions. (B) 2D interaction map of the most active compound **1** and GPR40.

In the case of AKR1B1, solutions of molecular docking into the catalytic site of this enzyme show that acid moieties of compounds **1, 2** and **3** interact with Tyr-48, His-110 and Trp-111 showed in several currently inhibitors of this enzyme, such as zopolrestat and tolrestat. Also, the naphthyl ring of **2**

228 conserves an interaction with Trp-111 through π–π stacking (Figure 5). All compounds showed moderate
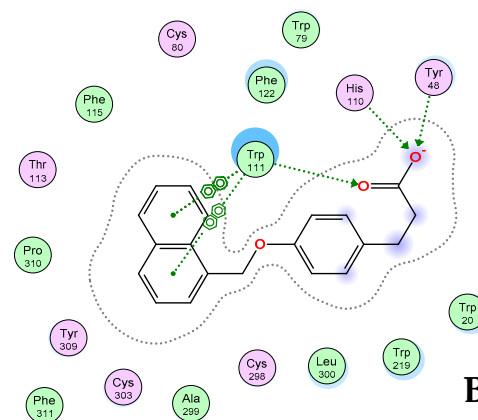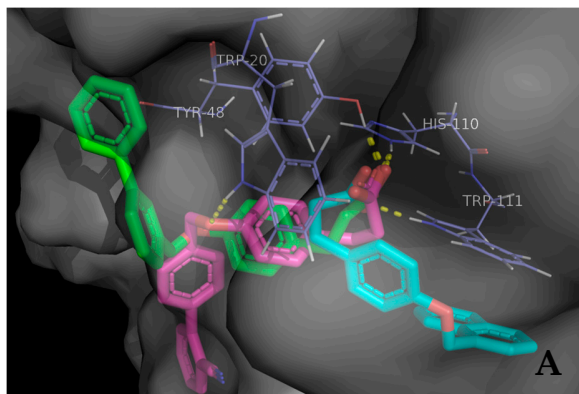229 in *vitro* inhibition of this enzyme.

230

Figure 5. 3D binding model of compounds **1-3** into the active site of Aldose reductase (AKR1B1).
Compounds **1** (green), **2** (cyan) and **3** (magenta) are shown as stick models. (B) 2D interaction map of the
second most active compound **2** and AKR1B1.

2.7. *In vivo* **antidiabetic effect of compounds 1-3**

235 Compounds **1-3** were the most active against some of targets identified as key elements in diabetes in
236 this work, and they were selected in order to evaluate their *in vivo* activity over Streptozotocin and
237 Nicotinamide diabetic induced mice, a well-known non insulin-dependent diabetes mellitus murine
238 model [7, 17]. Glibenclamide was used as a positive control, in order to ensure that the damage over β-
239 cells was partial and mice pancreas still produces insulin, that responds to a secretagogue such as
240 sulfonylurea drug used in this work. The antidiabetic activity of compounds **1-3** were determined using
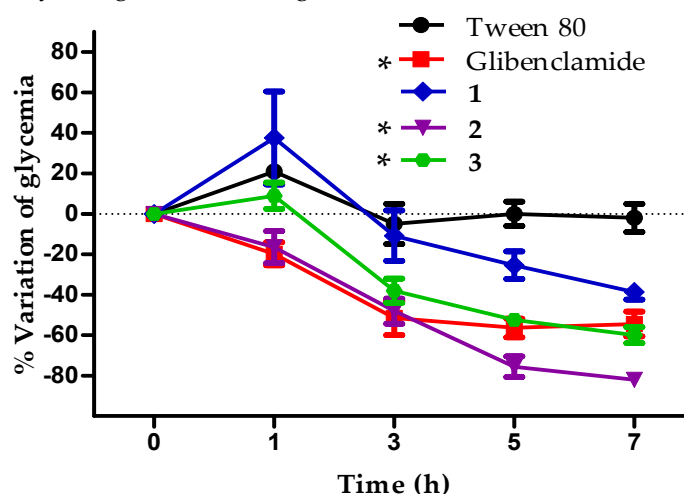241 a 100 mg/kg single dose, by intragastric route (Figure 6).

242

Figure 6. Effect of a single dose (100 mg/kg) of compounds **1-3** and glibenclamide (5 mg/kg) in
streptozotocin-nicotinamide-induced diabetes mice model (Intragastric, n = 6). *$p < 0.05$ versus Tween 80
(10%) group.

246   In the *in vivo* assay, compound **1** exhibited erratic pharmacokinetic behavior and poor antidiabetic effect
247   (Figure 6), and it could be explained by probable high degree of ionization at physiological pH, poor
248   permeability due to high ClogP (5.47), elevated protein binding, or susceptibility to phase 1
249   (hydroxylation) or phase 2 metabolism (glucuronidation). In particular, compounds **2** and **3** showed the
250   best *in vivo* activity, compared with **1** and control group (Tween 80). Compound **2** producing a sustained
251   decrease of blood glucose levels, close to 80% less, 7 h after compound administration (Figure 6). This
252   compound shown a statistically significant hypoglycemic effect like glibenclamide during the time that
253   the experiment lasted. The glucose lowering effect of compound **3** was increasing after the first hour of
254   administration (-20 % at 3 h, -50% at 5 h, and -60% at 7 h). Besides, statistically significant difference is
255   observed between **3** and tween 80 group, and the maximum effect was detected in the last hours of post-
256   intragastric administration (Figure 6).
257

258   **4. Materials and Methods**

259   **4.1. Chemistry**
260   All compounds and solvents were purchased from Sigma-Aldrich and were used without any further
261   purification. Melting points were determined using an EZ-Melt MPA120 automated apparatus from
262   Stanford Research Systems and are uncorrected. Reactions were monitored by TLC on 0.2 mm precoated
263   silica gel 60 F_{254} Merck plates. ^{1}H NMR spectra were recorded on Varian Oxford (600 MHz) and ^{13}C NMR
264   (150 MHz) instruments. Chemical shifts are given in ppm relative to Me_4Si, δ =0 in DMSO-d_6 and $CDCl_3$;
265   *J* values are given in Hz. The next abbreviations are used: s, singlet; d, doublet; q, quartet; dd, doublet of
266   doublet; t, triplet; m, multiplet; bs, broad signal. MS were recorded on a JEOL JMS-700 spectrometer by
267   electronic impact.

268   **4.2. General procedure for the synthesis of compounds 1-4.**
269   Ethyl esters **11-14** (0.70 mmol) were treated with a mixture of EtOH/H_2O (1:1, v/v) and KOH (2 equiv).
270   The mixture was stirred at reflux for 3-5 h. Subsequently, the ethanol was removed under vacuum and
271   HCl solution (10%, v/v) was added until reach pH 5, to obtain a precipitate which was filtered and
272   washed with cold water to give a solid. The crude products were recrystallized from ethanol or methanol
273   affording title compounds.

274   *4.2.1.* **3-[4-(Biphenyl-3-ylmethoxy)phenyl]propanoic acid (1)**: Yield 83%, pearly flakes Mp 123.7-126°C;
275   ^{1}H NMR (600 MHz, DMSO-*d6*) δ: 2.43 (t, 2H, CH_2), 2.74 (t, 2H, CH_2), 5.13 (s, 2H, CH_2), 6.94 (d, 2H, H-3A,
276   H-5A, J_0=7.74 Hz), 7.14 (d, 2H, H-2A, H-6A, J_0= 8.04 Hz), 7.4 (t, 1H, H-4C), 7.43 (d, 1H, H-4B, J_0=7.2 Hz),
277   7.48-7.46   (m, 3H, H-6B, H-3C, H-5C), 7.61 (t, 1H, H-5B, J_0=7.5 6Hz), 7.66 (d, 2H, H-2C, H-6C, J_0=8.22 Hz),
278   7.72 (s, 1H, H-2C) ppm. ^{13}C NMR (150 MHz, DMSO-*d6*) δ: 30.4 (CH_2), 36.9 (CH_2), 69.6 (O-CH_2), 115.1 (C-
279   3A, C-5A), 126.4 (C-6B), 126.6 (C-4B), 127.1 (C-2C, C-6C), 128 (C-4C), 129.4 (C-3C, C-5C), 129.5 (C-5B),
280   129.7 (C-2A, C-6A), 134 (C-1A), 138.5 (C-1C), 140.4 (C-1B), 140.8 (C-3B), 157.0 (C-4A), 174.7 (C=O) ppm.
281   MS/EI: m/z (% int. rel). 353 (M+Na), 178 (M+Na -175) 100%. Anal. Calcd for $C_{22}H_{20}O_3$: C 79.50, H 6.06;
282   Found C 79.54, H 6.04.

283   *4.2.2.* **3-[4-(1-Naphthylmethoxy)phenyl]propanoic acid (2)**: Yield 51%, white powder Mp 124.8-127.8°C;
284   ^{1}H NMR (600 MHz, DMSO-*d6*) δ: 2.49 (t, 2H, CH_2), 2.76 (t, 2H, CH_2), 5.50 (s, 2H, CH_2), 7.0 (d, 2H, H-3A,

285　　H-5A, J_o= 8.46 Hz), 7.16 (d, 2H, H-2A, H-6A, J_o= 8.46 Hz), 7.51 (t, 1H, H-3', J_o=7.56 Hz), 7.58-7.55　 (m, 2H,

286　　H-6', H-7'), 7.66 (d, 1H, J_o = 6.9 Hz), 7.92 (d, 1H, J_o = 8.52 Hz), 7.97 (d, 1H, J_o= 7.86 Hz), 8.08 (d, 1H, J_o=7.97

287　　Hz). δ: ^{13}C NMR (150 MHz, DMSO-*d6*) **δ**: 30.0 (CH$_2$), 36.1 (CH$_2$), 68.2 (CH$_2$), 115.1 (C-3A, C-5A), 124.3 (C-

288　　8'), 125.8 (C-3'), 126.4 (C-6'), 126.9 (C-7'), 127.03 (C-2'). 128.9 (C-5'), 129.0 (C-4'), 129.7 (C-2A, C-6A), 131.6

289　　(C-8a), 133.1 (C-1A), 133.6 (C-4a), 133.7 (C-1'), 157.2 (C-4A, 174.3 (C=O). MS/EI: m/z (% int. rel). 306 (M$^+$),

290　　141(M-165)100%. Anal. Calcd for C$_{20}$H$_{18}$O$_3$: C 78.41, H 5.92; Found C 78.43, H 5.91.

291　　***4.2.3. 3-{4-[(2'-Cyanobiphenyl-4-yl)methoxy]phenyl} propanoic acid (3).*** Yield 85%, pearly flakes m.p

292　　174-176.9; ^{1}H NMR (600 MHz, CDCl$_3$) δ: 2.66 (t, 2H, CH$_2$), 2.91 (t, 2H, CH$_2$), 5.11 (s, 2H, CH$_2$), 6.93 (d, 2H,

293　　H-3A, H-5A, J_o=8.52 Hz), 7.15 (d, 2H, H-2A, H-6A, J_o=8.46 Hz), 7.44 (t, 1H, H-4C, J_o=7.68 Hz), 7.51 (d,

294　　1H, H-6C, J_o=7.86 Hz), 7.55 (2H, H-3B, H-5B, J_o=8.22 Hz), 7.58 (2H, H-2B, H-6B, J_o=8.16 Hz), 7.63 (t, 1H,

295　　H-5C, J_o=7.62 Hz), 7.76 (d, 1H, H-3C, J_o=7.74 Hz), 12.10 (s, 1H, OH) ppm. ^{13}C NMR (150 MHz, CDCl$_3$)　δ:

296　　29.8 (CH$_2$), 35.9 (CH$_2$), 69.6 (CH$_2$), 111.3 (C-2C), 118.6 (CN), 114.9 (C-3A, C-5A), 127.6 (C-4C), 127.7 (C-

297　　3B,C-5B), 　129 (C-2B, C-6B), 129.3 (C-2A, C-6A), 130.0 (C-6C), 132.8 (C-5C), 133.8 (C-3C), 137.7 (C-4B),

298　　137.8 (C-1B), 145.1 (C-1C), 157.2 (C-4A), 178.7 (C=O) ppm. MS/EI: m/z (% int. rel). 355 (M$^+$), 192 (M-165)

299　　100%. Anal. Calcd for C$_{23}$H$_{19}$NO$_3$: C 77.29, H 5.36, N 3.92; Found C 77.31, H 5.34, N 3.94.

300　　***4.2.4. 3-[4-(Quinolin-3-ylmethoxy)phenyl]propanoic acid*** (**4**). Yield 95%, yellow crystals m.p 125.8-

301　　128.4°C; ^{1}H NMR (600 MHz, DMSO-*d6*) δ: 2.49 (t, 2H, CH$_2$), 2.74 (t, 2H, CH$_2$), 5.33 (s, 2H, CH$_2$), 6.97 (d,

302　　2H, H-3A, H-5A, J_o=8.82 Hz), 7.15 (d, 2H, H-2A, H-6^a, J_o=8.34 Hz), 7.62 (t, 1H, H-6', 　J_o=7.8, J_o= 7.14 Hz),

303　　7.66 (d, 1H, H-3', J_o=8.4 Hz), 7.79 (t, 1H, H-7', J_o=6.96, J_o=8.34 Hz), 7.99, d, 1H, H-5', J_o=8.16 Hz), 8.02 (d,

304　　1H, H-4', J_o=8.46 Hz), 8.41, d, 1H, H-8', J_o=8.52 Hz), 12.1 (s, 1H, OH) ppm. ^{13}C NMR (150 MHz, DMSO-

305　　*d6*) δ: 29.9 (CH$_2$), 35.9 (CH$_2$), 71.2 (CH$_2$), 115.1 (C-3A, C-5A), 119.9 (C-3'), 127.01 (C-6'), 128.4 (C-4a), 129.0

306　　(C-7'), 129.8 (C-2A, C-6A), 130.3 (C-5'), 133.8 (C-1A), 137.5 (C-4'), 147.4 (C-8a), 156.9 (C-4A), 158.2 (C-2'),

307　　174.2 (C=O) ppm. MS/EI: m/z (% int. rel). 307 (M$^+$) 100%, 142 (M-165) 75%. Anal. Calcd for C$_{19}$H$_{17}$NO$_3$: C

308　　74.25, H 5.58, N 4.56; Found C 74.20, H 5.52, N 4.56.

309　　**4.3. Synthesis of 3-{4-[2-(1,3-benzothiazol-2-ylamino)-2 oxoethoxy]phenyl}propanoic acid (5).**

310　　A mixture of *N*-1,3-benzothiazol-2-yl-2-chloroacetamide **15** (0.0006 mol), 3-(4-hydroxyphenyl)propanoic

311　　acid **9**　(1 equiv.), potassium carbonate (3 equiv.), potassium iodide (10 % mol) in 2 mL of acetonitrile

312　　was refluxed with continuous stirring. The reaction solvent was dried and the mixture was basified at

313　　pH= 3 with HCl 10 % (v/v). The solid was filtered off and dried to afford the corresponding compound.

314　　Yield 27%, low melting point solid; ^{1}H NMR (600 MHz, DMSO-*d-6*) δ: 2.41 (t, CH$_2$, H-2), 2.70 (t, CH$_2$, H-

315　　3), 4.78 (s, CH$_2$, H-4), 7.00 (t, H-5A, J_o =7.74 Hz), 7.20 (t, H-6A, J_o= 7.68 Hz), 7.32 (d, H-2, H-6B, J_o= 8.64

316　　Hz), 7.45 (s, H-3B, H-5B), 7.64 (d, H-4A, H-7A, J_o=7.80 Hz). ^{13}C NMR (150 MHz, DMSO-*d-6*) δ: 19.24 (C-

317　　3), 35.09 (C-2), 65.00 (C-4), 119.47 (C-4B), 120.16　(C-1B), 122.86 (C-4A, C-7A), 125.98 (C-3B, C-5B), 125.99

318　　(C-2B, C-6B), 130.55 (C-5A, C-6A), 134.17 (C-7A), 134.29 (C-3A), 136.06 (C-2 A), 157.95 (C-5), 171.56 (C-1);

319　　MS-ESI: m/z 357 (M + H$^+$). Anal. Calcd for C$_{18}$H$_{16}$N$_2$O$_4$S: C 60.66, H 4.53, N 7.86; Found C 60.71, H 4.54, N

320　　7.84.

321　　**4.4. Synthesis of (2E)-3-(4-hydroxyphenyl)acrylic acid** (**8**).

322　　4-Hydroxybenzaldehyde **6** (0.25 g, 2.04 mmol), β-alanine (0.1 equiv, 0.20 mmol) and malonic acid **7** (0.21g,

323　　1.1 equiv, 2.06 mmol) were suspended in pyridine (5 mL), following Knoevenagel reaction with

324　　subsequent decarboxylation. The flask was shaken well and heated under microwave irradiation system

325   (CEM Discovery Microwave System apparatus, 2450 MHz, 300 W) fitted with reflux condenser for 10

326   min   at 70 ° C. After irradiation, the mixture was poured onto cold water and acidified until pH 5. The

327   precipitate was collected by filtration, washed with water, dried and recrystallized from ethanol. Yield

328   80 %, yellow crystals Mp 214°C (dec); ^{1}H NMR (600 MHz, DMSO-*d6*) δ: 6.35 (d, 1H, =CH trans, *J*= 16 Hz),

329   6.86 (d, 2H, H-3′, H-5′, *Jo*=8.4 Hz), 7.55 (d, 2H, H-2′, H-6′, *Jo*= 8.4 Hz),   7.58 (d, 1H, =CH trans, *J*= 16 Hz),

330   8.87 (bs, 2H, OH, COOH) ppm.^{13}C NMR (150 MHz, DMSO-*d6*) δ: 115.4 (C-2), 116.2 (C-3′, C-5′), 126.1 (C-

331   1′), 130.4 (C-2′, C-6′), 145.3 (C-3),   158.3 (C-4′), 168.6 (C=O) ppm. MS/EI: *m/z* (% int. rel). 164 (M$^+$).

332   **4.5. Synthesis of 3-(4-hydroxyphenyl)propanoic acid (9).**

333   A mixture of acid **8** (0.2 g, 1.20 mmol) and Pd/C 10% (0.02 g) in ethanol (40 mL) was reduced with H$_2$ at

334   60 lb/in^2 in a hydrogenation apparatus for 30 min. After filtration and evaporation of the solvent uder

335   reduce pressure a yellow oil was obtained. After cooling, a solid compound (0.2 g, 99 % yield) was

336   obtained which purificated by recrystallyzation in ethanol. Yield 99 %, yellow crystals Mp 129-131°C; ^{1}H

337   NMR (600 MHz, DMSO-*d6*) δ:2.45 (t, 2H, CH$_2$), 2.72 (t, 2H, CH$_2$), 6.65 (d, 2H, H-3′, H-5′, *Jo*=8.01 Hz), 7.05

338   (d, 2H, H-2′, H-6′, *Jo*= 8.02 Hz), 9.54 (bs, 2H, OH, COOH) ppm.^{13}C NMR (150 MHz, DMSO-*d6*) δ: 30.1

339   (CH$_2$), 36.9 (CH$_2$), 115.5 (C-3′, C-5′), 129.5 (C-2′, C-6′), 131.8 (C-1′), 155.5 (C-4′), 175.1 (C=O) ppm. MS/EI:

340   *m/z* (% int. rel). 166 (M$^+$).

341   **4.6. Synthesis of ethyl 3-(4-hydroxyphenyl)propanoate (10)**

342   To a stirred solution of acid **9** (3 g, 18 mmol) in 30 mL of ethanol, under ice-cooling, was added thionyl

343   chloride (1.1 eq, 1.44 mL, 19 mmol) dropwise over 20 minutes. After stirring the reaction mixture for 3 h

344   at room temperature, methanol is distilled out and 25 mL of water is added. The separated ester is

345   extracted with ethyl acetate and washed with 10 mL of saturated sodium bicarbonate solution.

346   Evaporation of the ethyl acetate gave the ester in pure form. Yield 94%, yellow liquid; ^{1}H NMR (600 MHz,

347   CDCl$_3$) δ: 1.22 (d, 3H, CH$_3$), 2.59 (t, 2H, CH$_2$), 2.87 (t, 2H, CH$_2$), 4.12, q, 2H, CH$_2$), 6.74 (d, 2H, 2.09, 6.48,

348   H-3A-H-5A), 7.03 (d, 2H, 6.54, H-2A, H-6A). ^{13}C NMR (150 MHz, CDCl$_3$) δ: 14.2 (CH$_3$), 30.2 (CH$_2$), 36.3

349   (CH$_2$), 60.6 (CH$_2$), 115.4 (C-3A, C-5A), 129.4 (C-2A, C-6A), 154.3 (C-4A), 173.6 (C=O). MS/EI: m/z (% int.

350   rel). 194 (M$^+$) 49 %, 142 (M-74) 100%.

351   **4.7.General procedure for the synthesis of compounds 11-14**

352   A solution of ethyl 3-(4-hydroxyphenyl)propanoate **10** (0.5 g, 2.5 mmol) and K$_2$CO$_3$ (0.71 g, 5.1 mmol, 2

353   equiv) in appropriate polar aprotic solvent (5 mL acetonitrile or acetone) was heated at 40°C for 30

354   minutes. Adequately substituted methylaryl halides (1.1 equiv.) were added dropwise. The mixture was

355   heated to reflux for 8 h. The solvent was removed under reduced pressure. Cold water (10 mL) was added

356   and the mixture was stirred for 15 min. The resulting emulsion was extracted with ethyl acetate (3 x 15

357   mL). The solvent was removed *in vacuo* to give an oily product, which were purified by column

358   chromatography.

359   **4.7.1. Ethyl 3-[4-(biphenyl-3-ylmethoxy)phenyl] propanoate (11).** Yield 65%,   colorless liquid; ^{1}H NMR

360   (600 MHz, CDCl$_3$) δ: 1.21 (t, 3H, CH$_3$), 2.58 (t, 2H, CH$_2$), 2.88 (t, 2H, CH$_2$), 4.11 (c, 2H, CH$_2$′), 5.08 (s, 2H,

361   CH$_2$), 6.92 (d, 2H, Jo= 7.8, H-3A, H-5A), 7.11 (d, 2H, Jo= 8.1, H-2A, H-6A), 7.34 (t, 1H, Jo= 7.56, H-5B), 7.39

362   (d, 1H, 7.44, H-6B), 7.43-7.41 (m, 3H, H-3C, H-4C, H-5C), 7.54 (d, 1H, *Jo*= 7.68, H-4B), 7.58, d, 2H, *Jo*= 7.68,

363   H-2C, H-6C), 7.64 (s, 1H, H-2B) ppm. ^{13}C NMR (150 MHz, CDCl$_3$) δ: 14.2(CH$_3$), 30.1 (CH$_2$), 36.2 (CH$_2$),

364 60.3 (CH$_2$'), 70.1 (CH$_2$), 114.9 (C-3A, C-5A), 126.2 (C-4B), 126.3 (C-2B), 126.7 (C-BB), 127.2 (C-2C, C-6C),

365 127.4 (C-5B), 128.9 (C-3C, C-5C), 129 (C-4C), 129.3 (C-2A, C-6A), 133.0 (C-1A), 137.7 (C-1C), 140.9 (C-1B),

366 141.5 (C-3B), 157.2 (C-4A), 172.9 (C=O) ppm.   MS/EI: m/z (% int. rel).   360(M$^+$) 31 %, 167(M-193) 100%.

367 **4.7.2. Ethyl 3-[4-(1-naphthylmethoxy)phenyl]propanoate (12)**. Yield 78 %, colorless liquid; ^{1}H NMR (600

368 MHz, CDCl$_3$) δ:1.23 (t, 3H, CH$_3$), 2.59 (t, 2H, CH$_2$) 2.90 (t, 2H, CH$_2$) 4.12 (c, 2H, CH$_2$'), 5.44 (s, 2H, CH$_2$),

369 6.97 (d, 2H, 7.14, H-3A, H-5A) 7.14 (d, 2H, J_o= 7.68, H-2A, H-6A) 7.44 (t, J_o= 8.22, J_o= 8.28, H-3') 7.52-7.49

370 (m, 2H, H-6', H-7') 7.57 (d, 1H, J_o= 6.9, H-2') 7.83 (d, 1H, J_o= 8.22, H-4') 7.85 (d, 1H, J_o= 7.5, H-5') 8.03 (d,

371 J_o= 7.86, H-8') ppm. ^{13}C NMR (150 MHz, CDCl$_3$) δ: 14.2 (CH$_3$), 30.2 (CH$_2$), 36.2 (CH$_2$), 60.4 (CH$_2$'), 68.7

372 (CH$_2$), 114.9 (C-3A, C-5A), 123.7 (C-8'), 125.3 (C-3'), 125.9 (C-6'), 126.5 (C-7'), 128.7 (C-2'), 128.9 (C-5'),

373 129.3 (C-2A, C-6A), 131.5 (C-4'), 132.4 (C-8a), 133.1 (C-4a), 133.7 (C-1'), 157.4 (C-4a), 172.9 (C=O) ppm.

374 MS/EI: m/z (% int. rel). 334 (M$^+$) 11 %, 141(M-193) 100%.

375 **4.7.3. Ethyl 3-{4-[(2'-cyanobiphenyl-4-yl)methoxy] phenyl}propanoate (13).** Yield 64%, white crystals;

376 ^{1}H NMR (600 MHz, DMSO-*d6*) δ: 1.14 (t, 3H, CH$_3$), 2.56 (t, 2H, CH$_2$) 2.78 (t, 2H, CH$_2$) 4.03, c, 2H, CH$_2$'),

377 5.16 (s, 2H, CH$_2$) 6.96 (d, 2H, J_o= 8.04, H-3A, H-5A) 7.15 (d, 2H, J_o= 8.04, H-2A, H-6A), 7-64-7.60 (m, 6H,

378 H-2A, H-3A, H-5A, H-6A, H-4C, H-6C), 7.79 (t, 1H, J_o= 7.56, H-5C) 7.95 (d, 1H, J_o= 7.68, H-3C) ppm. ^{13}C

379 NMR (150 MHz, DMSO-*d6*) δ:14.5 (CH$_3$), 29.1 (CH$_2$), 35.8 (CH$_2$), 60.2 (CH$_2$'), 69.1 (CH$_2$), 110.6 (C-2C), 115

380 (H-3A, H-5A), 119 (CN), 128.7 (C-4C), 129.2 (C-2B, C-6B), 129.7 (C-2A, C-6A), 130.5 (C-6C), 133.2 (C-1A),

381 134 (C-5C), 134.3 (C-3C), 137.7 (C-4B), 138.3 (C-1B), 144.7 (C-1C), 157.2 (C-4A), 172.5 (C=O) ppm.   MS/EI:

382 m/z (% int. rel). 385 (M$^+$) 11%, 192(M-193) 100%.

383 **4.7.4. Ethyl 3-[4-(quinolin-2-ylmethoxy)phenyl]propanoate (14)**. Yield 72%, yellow liquid; ^{1}H NMR (300

384 MHz, CDCl$_3$) δ: 1.47 (t, 3H, CH$_3$), 2.50 (t, 2H, CH$_2$), 2.75 (t, 2H, CH$_2$), 4.01 (c, 2H, CH$_2$), 5.32 (s, 2H, CH$_2$),

385 6.96 (d, 2H, J_o= 6.66, J_o= 8.67, H-3A, H-5A), 7.13 (d, 2H, J_o= 8.58, H-2A, H-6A), 7.62, (d, 1H, J_o= 7.35, H-

386 6'), 7.65 (d, 1H, J_o= 8.49, H-3'), 7.79 (dd, 1H, J_o= 8.28, H-7'), 7.97 (dd, 1H, J_o= 8.85, H-5'), 8.01 (dd, 1H, J_o=

387 8.64, H-4'), 8.39 (d, 1H, 8.55, H-8') . ^{13}C NMR (75 MHz, CDCl$_3$) δ: 14.0 (CH$_3$), 29.4 (CH$_2$), 35.4 (CH$_2$), 59.7

388 (CH$_2$'), 70.7 (CH$_2$), 114.6 (C-3A, C-5A), 119.5 (C-3'), 127.1 (C-6'), 128.1 (C-4'), 128.5 (C-4a), 129.1 (C-7'),

389 129.8 (C-2A, C-6A), 130.5 (C-5'), 132.9 (C-1A), 137.9 (C-8'), 146.9 (C-8a), 158.7 (C-2'),   172.1 (C=O) ppm.

390 MS/EI: m/z (% int. rel).   335 (M$^+$) 10%.

391 *4.8.* **Synthesis of N-1,3-benzothiazol-2-yl-2-chloroacetamide (15).**

392 A mixture 2-amino-1,3-benzothiazol (0.100 g) and sodium bicarbonate (3 equiv.) was dissolved in acetone

393 (10 mL) and was stirred at room temperature. After 30 min, chloroacetyl chloride (1.5 equiv.) was added

394 dropwise using a drop funnel apparatus and stirred for 8 h. After the reaction was completed, the solvent

395 was removed under reduced pressure, and the precipitated white solid was washed with cold water.

396 Yield: 90 %, mp: 156.5-159.3°C; ^{1}H NMR (600 MHz, CDCl$_3$) δ: 4.32 (s, CH$_2$), 7.36 (t, H-6, J_o=8.10 Hz), 7.48

397 (t, H-5, J_o= 8.28 Hz), 7.84 (q, H-4, H-7, J_o=7.92 Hz); MS-EI: m/z 225.75 (M$^+$)40%, 149.61(M-77) 100%.

398 **4.3. Biological assays.**

399 *4.3.1.* **GPR40 agonistic activities of compounds 1-5**

400 This bioassay was previously described [2]. Briefly: About 4×10^4 hGPR40/HEK293 per well were seeded

401 in 96-well plate. After culturing for 24 h, cells were loaded with 2 μmol/L Fluo-4 AM in Hanks' balanced

402 salt solution at 37°C for 40 minutes. After thorough washing with 50 μL assay buffer, 25 μL assay buffer

403   containing compound was dispensed into the well, using a FlexStation III microplate reader and
404   intracellular calcium change was recorded with an excitation wavelength of 485 nm and emission
405   wavelength of 525 nm.

406   **4.3.2. Aldose reductase (AKR1B1) inhibition assay**

407   Human recombinant AKR1B1 was purified to electrophoretic homogeneity as previously described [24].
408   The enzymatic activity was measured at 37 °C following the decrease of absorbance at 340 nm. The assay
409   mixture (final volume 0.7 mL) contained, in 0.25 M sodium phosphate buffer pH 6.8, 4.67 mM D,L-
410   glyceraldehyde, 0.11 mM NADPH, 0.38 M $(NH_4)_2SO_4$ and 0.5 mM EDTA. One Unit of enzyme activity
411   refers to the amount of enzyme that catalyses the oxidation of 1 μmol/min of NADPH in the above
412   conditions. Compounds **1-5**, tested as AKR1B1 inhibitors were dissolved at proper concentrations in a
413   mixture DMSO/methanol (40:60, v/v) and added to the above described assay mixture containing 5 mU
414   of purified AKR1B1; the concentrations of DMSO and methanol in all the assays were kept constant at
415   0.2 and 0.3% (v/v), respectively. IC_{50} values was determined by nonlinear regression analysis by fitting
416   the data to the equation describing one site competition in a log concentration-inhibition curve. For each
417   curve, at least five different concentrations of inhibitor were analyzed [25].

418   **4.3.3. In vitro PPARγ and GLUT-4 assay**

419   Both assays were performed as previously described [7, 17, 29-31]. Briefly: 3T3-L1 fibroblasts ($9×10^5$ cells
420   per well) were cultured in 6-well plates in Dulbecco's modified Eagle's medium. After 2 days of
421   confluence, the cells were differentiated to the adipocyte phenotype with 0.5 mM 3-isobutyl-1-
422   methylxanthine, 0.25 μM dexamethasone acetate, and 0.8 μM insulin, for 48 h, followed by insulin alone
423   for other 48 h. To determine the effect of compounds on PPARγ and GLUT-4 expression, the cells were
424   treated by 24 h. RNA was isolated from cultured cells and two μg of total RNA were reverse-transcribed
425   in a thermocycler. The enzyme was inactivated and finally samples were cooled. Then 1/10 volume of
426   each reverse-transcribed reaction was amplified with SYBR Green master mix containing 0.5 mM of
427   customized primers for PPAR-γ and GLUT-4. PCR was conducted and the threshold cycles (Ct) were
428   measured in separate tubes and in duplicate. The ΔCt values were calculated in every sample for each
429   gene of interest. Relative changes in the expression level of one specific gene (ΔΔCt) were calculated [31].

430   **4.4. In vivo Assay**

431   CD1 mice (20-25 g) were housed in groups of six (n = 6) under laboratory conditions. Before
432   experimentation, all animals were fasted for 16 h with water *ad libitum*. All animal procedures were
433   conducted in accordance with the Mexican Federal Regulations for Animal Experimentation and Care.
434   Acute antidiabetic assay: Non-insulin-dependent diabetes mice model was induced in overnight fasted
435   mice by a single i.p. injection of 100 mg/kg STZ, 15 min before the i.p. administration of 40 mg/kg of
436   nicotinamide. Hyperglycemia was confirmed by the higher glucose concentration in plasma, determined
437   at 2 weeks by glucometer. The animals with blood glucose concentration higher than 200 mg/dL were
438   used for the screening [32-35]. The diabetic animals were divided into three groups of six animals each
439   (n=6). Mice of experimental groups were administered a suspension of the compounds **1-3** (100 mg/kg,
440   prepared in 10% tween 80). Control group animals were also treated with 10 % tween 80. Glibenclamide
441   (5 mg/kg) was used as hypoglycemic reference drug. Blood samples were collected from the caudal vein
442   at 0, 1, 3, 5 and 7 h after administration. Blood glucose concentration was estimated using a commercial

443   glucometer [35-37]. The percentage variation of glycemia for each group was calculated. All values were
444   expressed as mean ± S.E.M. Statistical significance was estimated by analysis of variance (ANOVA).

4.5. In silico docking studies

446   The crystal structures of PPARγ, GPR40 and aldose reductase were retrieved from the PDB with the
447   accession codes: 1I7I, 4PHU and 1Z3N respectively. Docking calculations were conducted with
448   AutoDock, version 4.2. The program performs several runs in each docking experiment. Each run
449   provides one predicted binding mode. All water molecules and every co-crystall ligands were removed
450   from the crystallographic structure and all hydrogen atoms were added. For all ligands and proteins,
451   Gasteiger charges were assigned and non-polar hydrogen atoms were merged. All torsions could rotate
452   during docking. The auxiliary program AutoGrid generated the grid maps. Each grid was centered at
453   the crystallographic coordinates of the crystallographic compound with dimensions of 60 x 60 x 60 Å
454   with points separated by 0.375 Å. The number of docking runs was 100. After docking, all solutions were
455   clustered into groups with RMSD lower than 2.0 Å. Discovery Studio version 3.5, Pymol version 1.0 and
456   MOE [38] were used for visualization.

4.5.1. Docking Validation

458   The molecular docking protocols were validated by re-docking of co-crystal ligands into the active site
459   of the structure of each protein target: PPARγ (Tesaglitazar), GPR40 (TAK-875) and aldose reductase
460   (Lidorestat). The RMSD between the co-crystal ligand and the docked structure was less than 2.0 Å in all
461   cases. This value indicates that the parameters for docking simulations are good in reproducing
462   orientation and conformation in the X-ray crystal structure of enzyme and receptors.

5. Conclusions

464   Five phenylpropanoic acid derivatives active on different relevant targets involved in the control of
465   glucose level and in the cell damage linked to hyperglycaemic conditions, are presented as promising
466   antidiabetic compounds. In fact, compounds **1** to **3** are able with different effectiveness to combine a
467   significantly increase in the mRNA expression of PPARγ, GLUT-4, with a GPR40 agonist action and a
468   well detectable inhibition of the AKR1B1 activity. Compounds **2** and **3** also revealed their antidiabetic
469   effectiveness *in vivo*, showing a robust hypoglycemic effect similar to glibenclamide. The *in vitro*
470   satisfactory multitargeting anti-diabetic profile and the *in vivo* hypoglycemic activity make them suitable
471   leads in developing new chemical entities with polypharmacological ability to be used for treatment of
472   diabetes and its complications. To our knowledge, this is the first study reporting a multiple combined
473   action of a single molecule facing towards four relevant targets involved into cellular glucose handling.

483   **Author Contributions:** B. Colín-Lozano: performed the chemical synthesis of all compounds, did the acquisition of
484   antidiabetic *in vitro* and *in vivo* data, and analyzed the chemical and biological results. S.Estrada-Soto, F. Chavez
485   Silva and L. Cerón Romero: Carried out and interpreted the antidiabetic assays. A. Gutierrez-Hernandez:
486   performed and analyzed the *in silico* refined molecular docking in to the PPARγ, GPR40 and AKR1B1. A. Giacoman-
487   Martinez and J. C. Almanza-Perez: Conducted and interpreted the *in vitro* relative expression of PPARγ and GLUT-
488   4 experiments. E. Hernández-Núñez: performed and interpreted the spectroscopic analysis using nuclear magnetic
489   resonance in 1 and 2 dimensions. He also wrote the Supplementary Information. Z. Wang and X. Xie: performed
490   and supervised the *in vitro* GPR40 experiments and edited the manuscript. M. Capiello, F. Balestri and U. Mura:
491   performed the *in vitro* aldose reductase inhibition assay, interpreted the data for SAR analysis, contributed with
492   reagents and analysis tools, drafted some parts of the manuscript and did a critical revision. G. Navarrete-Vázquez:
493   Developed the concept, designed the compounds, analyzed and interpreted data, prepared and wrote the
494   manuscript.

495   **Conflicts of Interest:** The authors declare no conflict of interest.

496   **References**

497   1. Schwartz, S. S.; Epstein, S.; Corkey, B. E.; Grant, S.F.;   Gavin 3rd, J.R.; Aguilar, R.B. The Time Is Right for a New
498   Classification System for Diabetes: Rationale and Implications of the β-Cell-Centric Classification Schema.
499   *Diabetes Care*. **2016**, *39*, 179-186.

500   2. Huang, J.; Guo, B.; Chu, W.J.; Xie, X.; Yang, Y. S.; Zhou, X.L. Design, synthesis and evaluation of potent G-protein
501   coupled receptor 40 agonists. *Chin. Chem. Lett*. **2016**, 27**,** 159-162.

502   3. Edfalk, S.; Steneberg, P.; Edlund, H. GPR40 is expressed in enteroendocrine cells and mediates free fatty acid
503   stimulation of incretin secretion. *Diabetes* **2008**, *57,* 2280-2287.

504   4. Mancini, A. D.; Poitout, V. The fatty acid receptor FFA1/GPR40 a decade later: how much do we know? *Trends*
505   *Endocrinol. Metab*. **2013**, *24*, 398-407.

506   5. Morgan, N.G.; Dhayal, S. G-protein coupled receptors mediating long chain fatty acid signalling in the pancreatic
507   beta-cell. *Biochem. Pharmacol*. **2009**, *78*, 1419-1427.

508   6. Chen, C.; Li, H.; Long, Y.Q.   GPR40 agonists for the treatment of type 2 diabetes mellitus: The biological
509   characteristics and the chemical space. *Bioorg. Med. Chem. Lett*. **2016**, *26,* 5603-5612.

510   7. Navarrete-Vázquez, G.; Torres-Gómez, H.; Hidalgo-Figueroa, S.; Ramírez- Espinosa, J.J.;   Estrada-Soto, S.;
511   Medina-Franco, J.L.; León-Rivera, I.; Alarcón-Aguilar, F.J.; Almanza-Pérez, J.C. Synthesis, in vitro and in silico
512   studies of a PPARγ and GLUT-4 modulator with hypoglycemic effect .*Bioorg. Med. Chem. Lett*. **2014, 24,** 4575-
513   4579.

514   8. Meinke, P.T.; Wood, H.B.; Szewczyk, J.W. Nuclear hormone receptor modulators for the treatment of diabetes
515   and dyslipidemia. *Annu. Rep. Med. Chem*. **2006**, *41,* 99-126.

516   9. Nevin, D.K.; Lloyd, D.G.; Fayne, D. Rational targeting of peroxisome proliferating activated receptor subtypes.
517   *Curr. Med. Chem*. **2011**, *18*, 5598-5623.

518   10. Sternbach, D.D. Modulators of the peroxisome proliferator-activated receptors (PPARs). *Annu. Rep. Med. Chem*.
519   **2003**, *38*, 71-80.

520   11. Yasmin, S.; Jayaprakash, V. Thiazolidinediones and PPAR orchestra as antidiabetic agents: From past to present.
521   *Eur. J. Med. Chem*. **2016**, *126*, 879-893.

522   12. Balestri, F.; Cappiello, M.; Moschini, R.; Rotondo, R.; Abate, M.;   Del Corso, A.; Mura, U.   Modulation of aldose
523   reductase activity by aldose hemiacetals. *Biochim. Biophys. Acta* **2015**, *1850,* 2329-2339.

524   13. Del Corso, A.; Cappiello, M.; Mura, U. From a dull enzyme to something else: facts and perspectives regarding
525   aldose reductase. *Curr. Med. Chem*. **2008**, *15,* 1452-1461.

526 14. Lee, A.Y.; Chung, S.S. Contributions of polyol pathway to oxidative stress in diabetic cataract *FASEB J.* **1999**, *13*,
527   23-30.

528 15. Hamada, Y.; Araki, N.; Koh, N.; Nakamura, J.; Horiuchi, S.; Hotta, N. Rapid formation of advanced glycation end
529   products by intermediate metabolites of glycolytic pathway and polyol pathway. *Biochem. Biophys. Res. Commun.*
530   **1996**, *228*, 539-543.

531 16. Briscoe, C.P.; Peat, A. J.; McKeown, S.C.; Corbett, D.F.; Goetz, A.S.; Littleton, T.R.; McCoy, D.C.;   Kenakin, T.P.;
532   Andrews, J.L.;   Ammala, C.; Fornwald, J.A.;   Ignar, D.M.;   Jenkinson, S. Pharmacological regulation of insulin
533   secretion in MIN6 cells through the fatty acid receptor GPR40: identification of agonist and antagonist small
534   molecules *Br. J. Pharmacol.* **2006**, *148*, 619-628.

535 17. Hidalgo-Figueroa, S.; Ramírez-Espinosa, J.J.; Estrada-Soto, S.; Almanza-Pérez, J.C.;   Román-Ramos, R.; Alarcón-
536   Aguilar, J.F.;   Hernández-Rosado, J.V.; Moreno-Díaz, H.; Díaz-Coutiño, D.; Navarrete-Vázquez, G. Discovery of
537   thiazolidine-2,4-dione/biphenylcarbonitrile hybrid as dual PPAR α/γ modulator with antidiabetic effect: in vitro,
538   in silico and in vivo approaches. *Chem. Biol. Drug Des.* **2013**, *81*, 474-483.

539 18. Wang, S.; Awad, K.S.; Elinoff, J.M.; Dougherty, E.J.; Ferreyra, G.A.; Wang, J.Y.; Cai, R.; Sun, J.; Ptasinska, A.;
540   Danner, R.L. G protein-coupled receptor 40 (GPR40) and peroxisome proliferator-activated receptor γ (PPARγ):
541   an integrated two-receptor signaling pathway *J. Biol. Chem.* **2015**, *290*, 19544-19557.

542 19. Reddy, T.N.; Ravinder, M.; Bagul, P.; Ravikanti, K.; Bagul, C.; Nanubolu, J.B.; Srinivas, K.; Banerjee, S.K.; Rao,
543   V.J. Synthesis and biological evaluation of new epalrestat analogues as aldose reductase inhibitors (ARIs). *Eur. J.*
544   *Med. Chem.* **2014**, *71*, 53-66.

545 20. Li, Y.; Qiang, X.; Luo, L.; Yang, X.;   Xiao, G.;   Zheng, Y.;   Cao, Z.; Sang, Z. ; Su, F.;   Deng, Y. Multitarget drug
546   design strategy against Alzheimer's disease: Homoisoflavonoid Mannich base derivatives serve as
547   acetylcholinesterase and monoamine oxidase B dual inhibitors with multifunctional properties. *Bioorg. Med.*
548   *Chem.* **2017**, *25*, 714-726.

549 21. Sasaki, S.;   Kitamura, S.; Negoro, N.;   Suzuki, M.; Tsujihata, Y.; Suzuki, N.; Santou, T.; Kanzaki, N.; Harada, M.;
550   Tanaka, Y.; Kobayashi, M.; Tada, N.; Funami, M.; Tanaka, T.; Yamamoto, Y.; Fukatsu, K.;   Yasuma, T.; Momose,
551   Y. Design, synthesis, and biological activity of potent and orally available G protein-coupled receptor 40 agonists.
552   *J. Med. Chem.* **2011**, *54*, 1365-1378.

553 22. Christiansen, E.; Due-Hansen, M.E.; Urban, C.; Merten, N.; Pfleiderer, M.; Karlsen, K.K.; Rasmussen, S.S.:
554   Steensgaard, M.; Hamacher, A.;   Schmidt, J.; Drewke, C.; Petersen, R.K.; Kristiansen, K.; Ullrich, S.; Kostenis, E.;
555   Kassack, M.U.; Ulven, T. Structure-Activity Study of Dihydrocinnamic Acids and Discovery of the Potent FFA1
556   (GPR40) Agonist TUG-469. *ACS Med. Chem. Lett.* **2010**, *1*, 345-349.

557 23. Negoro, N.; Sasaki, S.; Mikami, S.; Ito, M.; Tsujihata, Y.; Ito, R.; Suzuki, M.; Takeuchi, K.; Suzuki, N.;   Miyazaki,
558   J.; Santou, T.; Odani, T.; Kanzaki, N.; Funami, M.; Morohashi, A.; Nonaka, M.; Matsunaga, S.;   Yasuma, T.;
559   Momose, Y.   Optimization of (2,3-dihydro-1-benzofuran-3-yl)acetic acids: discovery of a non-free fatty acid-like,
560   highly bioavailable G protein-coupled receptor 40/free fatty acid receptor 1 agonist as a glucose-dependent
561   insulinotropic agent. *J. Med. Chem.* **2012**, *55*, 3960-3974.

562 24. Balestri, F.; Cappiello, M.; Moschini, R.; Rotondo, R.; Buggiani, I.; Pelosi, P.; Mura, U.; Del Corso,   A.   L-Idose:
563   an attractive substrate alternative to D-glucose for measuring aldose reductase activity. *Biochem. Biophys. Res.*
564   *Commun.* **2015**, *456*, 891-895.

565   25. Balestri, F.; Rotondo, R.; Moschini, R.; Pellegrino, M.; Cappiello, M.; Barracco, V.; Misuri, L.; Sorce, C.; Andreucci,
566   A.; Del-Corso, A.; Mura, U. Zolfino landrace (Phaseolus vulgaris L.) from Pratomagno: general and specific
567   features of a functional food. *Food. Nutr. Res.* **2016**, *60*, 31792.

568   26. Tsao, T.S.; Li, J.; Chang, K.S.; Stenbit, A.E.; Galuska, D.; Anderson, J.E.; Zierath, J.R.; McCarter, R.J.; Charron, M.J.
569   Metabolic adaptations in skeletal muscle overexpressing GLUT4: effects on muscle and physical activity. *FASEB*
570   *J.* **2001**, *15*, 958-969.

571   27. http://bio-hpc.ucam.edu/dia-db/

572   28. Sánchez-Pérez, A.; Muñoz, A.; Peña-García, J. ; den-Haan, H. ; Bekas N.; Katsikoudi, A.; Tzakos, A.G. ; Pérez-
573   Sánchez, H. DIA-DB: A Web-Accessible Database for the Prediction of Diabetes Drugs. *Bioinformatics and*
574   *Biomedical Engineering* **2015**, *9044*, **655-663.

575   29. García-Macedo, R.; Sánchez-Muñoz, F.; Almanza-Pérez, J.C.; Duran-Reyes, G.; Alarcón-Aguilar, F.; Cruz, M.
576   Glycine increases mRNA adiponectin and diminishes pro-inflammatory adipokines expression in 3T3-L1 cells.
577   *Eur. J. Pharmacol.* **2008**, *587*, 317-321.

578   30. Almanza-Pérez, J.C., Alarcón-Aguilar, F.J. ; Blancas- Flores, G.; Campos-Sepúlveda, A.E.; Román-Ramos, R.;
579   García-Macedo, R.; Cruz, M. Glycine regulates inflammatory markers modifying the energetic balance through
580   PPAR and UCP-2. *Biomed. Pharmacother.* **2010**, *64*, 534-540.

581   31. Hidalgo-Figueroa, S.; Navarrete-Vázquez, G.; Estrada-Soto, S.; Giles-Rivas, D.; Alarcón-Aguilar, F.J.; León-
582   Rivera, I.; Giacoman-Martínez, A.; Miranda-Pérez, E.; Almanza-Pérez, J.C. Discovery of new dual PPARγ-GPR40
583   agonists with robust antidiabetic activity: Design, synthesis and in combo drug evaluation. *Biomed. Pharmacother.*
584   **2017**, *90*, 53-61.

585   32. Verspohl, E. J. Recommended testing in diabetes research. *Planta Medica* **2002**, *68*, 581-590.

586   33. Goyal, S.N.; Reddy, N.M.; Patil, K.R.; Nakhate, K.T.; Ojha, S.; Patil, C.R.; Agrawal, Y.O. Challenges and issues
587   with streptozotocin-induced diabetes - A clinically relevant animal model to understand the diabetes
588   pathogenesis and evaluate therapeutics.*Chem. Biol. Interact.* **2016**, *244*, 49-63.

589   34. Hayashi, K.; Kojima, R.; Ito, M. Strain differences in the diabetogenic activity of streptozotocin in mice *Biol.Pharm.*
590   *Bull.* **2006**, *6*, 1110-1119.

591   35. Radenković, M.; Stojanović, M.; Prostran, M. Experimental diabetes induced by alloxan and streptozotocin: The
592   current state of the art. *J. Pharm. Toxicol. Methods* **2016**, *78*, 13-31.

593   36. Ortiz-Andrade, R.; Rodríguez-López, V.; Garduño-Ramírez, M.; Castillo-España, P.; Estrada-Soto, S. Anti-
594   diabetic effect on alloxanized and normoglycemic rats and some pharmacological evaluations of Tournefortia
595   hartwegiana. *J. Ethnopharmacol.* **2005**, *101*, 37-42.

596   37. Gutierrez-Lara, E.; Martínez-Conde, C.; Rosales-Ortega, E. Ramírez-Espinosa, J.J.; Rivera-Leyva,
597   J.C.; Centurión, D.; Carvajal, K.; Ortega-Cuellar, D.; Estrada-Soto, S.; Navarrete-Vázquez, G. Synthesis
598   and In Vitro AMPK Activation of Cycloalkyl/Alkarylbiguanides with Robust In Vivo Antihyperglycemic
599   Action. *J. Chem.* **2017,** *1212609*, 1-8.   https://doi.org/10.1155/2017/1212609

600   38. Molecular Operating Environment (MOE), 2016.08; Chemical Computing group ULC, 1010 Sherbooke St. West,
601   Site #910, Montreal, QC, Canada, H3A 2R7, **2018**. http://www.chemcomp.com

602   **Sample Availability:** Samples of the compounds are available from the authors.